

CubeSat Solid Rocket Motor Propulsion Systems providing Delta-Vs greater than 500 m/s

Kevin L. Zondervan, Jerry Fuller, Darren Rowen, Brian Hardy, Chris Kobel,
Shin-Hsing Chen, Phillip Morrison, Timothy Smith, and Alison Kremer
The Aerospace Corporation
2011 Crystal Dr, Suite 900, Arlington, VA 22202-3780; 571-447-3879
Kevin.Zondervan@aero.org

ABSTRACT

Over the past three years, a team at The Aerospace Corporation has been investigating high Delta-V solid rocket motor propulsion systems for CubeSats. All solid rocket motors have an unknown thrust misalignment. Therefore, any vehicle propelled by a solid rocket motor must include an attitude control system (ACS) capable of dealing with the torque generated by this thrust misalignment. We have designed and flight-tested two solid rocket motor thrust vector control (TVC) systems that provide the means for an ACS to null the thrust misalignment of a small solid rocket motor and allow the CubeSat to be steered while accelerating. The two TVC systems use completely different approaches -- one is a moving mass system, the other is a nozzle jet paddle system. The TVC systems can be combined with a small solid (or liquid) rocket motor to provide a 1U (a 10 cm cube) x 1 kg propulsion unit that can be attached to a 1 kg CubeSat and provide up to 950 m/s of Delta-V. The propulsion systems are highly scalable and can be designed to provide smaller or larger amounts of Delta-V as desired. A 2U (a 20 cm x 10 cm x 10 cm cuboid) x 2.5 kg propulsion unit attached to a 1 kg CubeSat can provide up to 1400 m/s of Delta-V. The proof-of-concept designs and flight tests of these propulsion systems are presented.

1. PROPULSION SYSTEM REQUIREMENTS FOR CUBESATS

Generally speaking, an on-orbit satellite needs a propulsion system to accomplish its mission. The functions performed by the propulsion system fall into

two broad categories: 1) orbit raising and transfers, where the ΔV can range from 60 to 4000 m/s, and 2) orbit maintenance and attitude control, where the ΔV is typically under 75 m/s per year. Typical propulsion system requirements associated with these functions are shown in Table 1¹.

Table 1: Typical Functions and Requirements for Space Propulsion

Propulsion Function	Typical Requirement
Orbit transfer to GEO (orbit insertion) • Perigee burn • Apogee burn	2,400 m/s 1,500 (low inclination) to 1,800 m/s (high inclination)
Initial spinup	1 to 60 rpm
LEO to higher orbit raising ΔV • Drag-makeup ΔV • Controlled-reentry ΔV	60 to 1,500 m/s 60 to 500 m/s 120 to 150 m/s
Acceleration to escape velocity from LEO parking orbit	3,600 to 4,000 m/s into planetary trajectory
On-orbit operations (orbit maintenance) • Despin • Spin control • Orbit correction ΔV • East-West stationkeeping ΔV • North-South stationkeeping ΔV • Survivability or evasive maneuvers (highly variable) ΔV	60 to 0 rpm ± 1 to ± 5 rpm 15 to 75 m/s per year 3 to 6 m/s per year 45 to 55 m/s per year 150 to 4,600 m/s
Attitude control • Acquisition of Sun, Earth, Star • On-orbit normal mode control with 3-axis stabilization, limit cycle • Precession control (spinners only) • Momentum management (wheel unloading) • 3-axis control during ΔV	3 to 10% of total propellant mass Low total impulse, typically <5,000 N-s, 1K to 10K pulses, 0.01 to 5.0 sec pulsewidth 100K to 200K pulses, minimum impulse bit of 0.01 N-s, 0.01 to 0.25 sec pulsewidth Low total impulse, typically <7,000 N-s, 1K to 10K pulses, 0.02 to 0.20 sec pulsewidth 5 to 10 pulse trains every few days, 0.02 to 0.10 sec pulsewidth On/off pulsing, 10K to 100K pulses, 0.05 to 0.20 sec pulsewidth

This paper presents two solid rocket motor (SRM) systems for accomplishing the high ΔV functions shown in Table 1 for very small satellites known as CubeSats. CubeSats are satellites of a standard cuboid shape with a mass generally under 10 kg. One side is required to be 10 cm x 10 cm, but the orthogonal dimension may be of variable length ranging typically from 5 cm to 30 cm. When the length is 10 cm and the volume is 1 liter, the CubeSat is denoted as a 1 unit or 1U CubeSat. When the length is 20 cm and the volume is 2 liters, the CubeSat is denoted as a 2U, and so on.

An SRM propulsion system provides a satellite a ΔV by thrusting for a period of time. Given the required ΔV , the required total impulse, I , of the propulsion system can be determined from three propulsion system parameters: the specific impulse I_{sp} , the propellant mass fraction (mass of propellant divided by initial mass of the propulsion system) f_p , and the mass of the payload, m_{pl} , which in this case is the mass of a CubeSat. We can write this relationship in the form of three equations:

$$I = I_{sp} g m_p \quad (1)$$

where m_p is the mass of the propellant and g is the standard value of gravity,

$$m_p = (m_{total} - m_{pl}) f_p \quad (2)$$

where m_{total} is the initial mass of the entire vehicle – the CubeSat and the propulsion system, and

$$m_{total} = \frac{m_{pl} f_p e^{\Delta V / (I_{sp} g)}}{1 - (1 - f_p) e^{\Delta V / (I_{sp} g)}} \quad (3)$$

The thrust of the propulsion system depends on its burn time, t_{burn} . The average thrust T is given by

$$T = I / t_{burn} \quad (4)$$

Typical values of specific impulse and propellant mass fraction of state-of-the-art solid rocket motors range from 185 sec to 280 sec, and 0.5 to 0.8, respectively. Larger motors typically have higher specific impulse and propellant mass fraction. Three typical SRMs are shown in Figure 1.

Assuming a CubeSat size SRM has a specific impulse of 277 sec and a propellant mass fraction of 0.6, and a larger SRM for specialized applications such as a LEO-to-GEO two-stage transfer vehicle has a specific impulse of 282 sec and a propellant mass fraction of 0.78, we can determine typical values of ΔV , total impulse I , and total initial vehicle mass m_{total} , for a

range of CubeSat sizes from 1 kg to 10 kg. The result is shown in Table 2.



	ISP 30 sec Motor	ATK STAR 4G	ATK STAR 12GV
Diameter, cm:	5.72	11.30	31.09
Length, cm:	24.93	13.79	57.15
Total Impulse, N-s:	997	2,657	91,200
Average Thrust, N:	37	258	6561
Burn Time, s:	27	10.3	13.9
Specific Impulse, s:	187	277	282
Initial Mass, kg:	0.95	1.50	42.0
Propellant Mass, kg:	0.54	0.98	32.9
Propellant Mass Frac:	0.57	0.65	0.78
TVC included?	NO	NO	YES

Figure 1: Typical Small Solid Rocket Motors

To summarize the results, the total impulse needed of a high ΔV SRM propulsion system, and its associated mass, for three representative applications is as follows:

- 1) 300 to 6,500 N-s (0.2 to 3.9 kg) for LEO in-plane orbit raising/lowering,
- 2) 2,700 to 27,000 N-s (1.6 to 16 kg) for 10 deg plane changes in LEO, and
- 3) 35,000 to 350,000 N-s (16.5 to 165 kg) for transfers from LEO to GEO.

Table 2: Typical CubeSat Total Impulse and Vehicle Mass to Perform an Orbit Maneuver

2nd Stage Isp, sec =	277
2nd Stage Propellant Mass Fraction =	0.60
1st Stage Isp, sec =	282
1st Stage Propellant Mass Fraction =	0.78
Fraction of ΔV provided by 1st Stage =	0.70

Propulsion Function	ΔV m/s	Rocket Stage Used	Total Impulse & Vehicle Mass		
			1 kg Payload	3 kg Payload	10 kg Payload
LEO Orbit Raising of 500 km	270	2nd	304 N-s 1.2 kg	913 N-s 3.6 kg	3,040 N-s 11.8 kg
LEO Orbit Raising of 1000 km	510	2nd	647 N-s 1.4 kg	1,940 N-s 4.2 kg	6,470 N-s 13.9 kg
10° Plane Change 1000 km Alt	1,281	2nd	2,680 N-s 2.6 kg	8,050 N-s 7.9 kg	26,800 N-s 26.2 kg
LEO (28.5° inc) to GEO (0° inc)	4,290	1st & 2nd	34,700 N-s 17.5 kg	104,000 N-s 52.4 kg	347,000 N-s 175 kg

2. STATE OF THE ART OF CUBESAT PROPULSION SYSTEMS

A large number of propulsion systems for CubeSats have recently emerged. A summary of 22 of these systems is shown in Figure 2, where they are ranked in terms of total impulse per unit volume². Noting that a 1U CubeSat has a volume of 1 liter, the graph can be considered the total impulse of the 22 propulsion systems scaled to a size of 1U. Six basic technologies are represented: electric thrusters, electrostatic thrusters, warm/cold gas systems, mono-propellant systems, SRMs, and electrolysis of water systems.

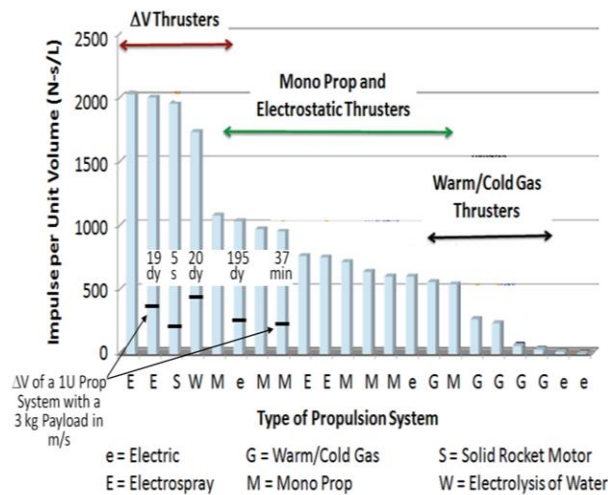


Figure 2: Total Impulse per Unit Volume of Some Current CubeSat Propulsion Systems

Also shown in Figure 2 for a few of the higher impulse systems are the ΔV and burn time (or thrust time) when fabricated to 1U (1 liter) in size and propelling a 3 kg payload. The current state-of-the-art covers a broad range of capabilities, and can provide the ΔV required for applications such as orbit raising/lowering (500 m/s), but not the ΔV for small plane changes (1300 m/s) and LEO-to-GEO transfers (4300 m/s). With one exception (an SRM system) all of these applications require long periods of time to complete, due to the low thrust of these systems. The times range from 37 min to 195 days.

For CubeSat missions requiring more timely orbit maneuvers, high- ΔV , high-thrust propulsion systems are required. SRMs are ideal for this application. So why is only one of the 22 systems shown in Figure 2 an SRM? One possible answer lies in the challenging requirements of attitude control systems for controlling high thrust propulsion systems.

3. THE CHALLENGE OF HIGH-THRUST, HIGH- DELTA-V PROPULSION SYSTEMS FOR CUBESATS

A rocket-propelled vehicle such as a satellite requires a system to point its thrust vector in a desired direction. An attitude control system (ACS) is used for this purpose. The thrust of the rocket system strongly influences the torque required of the ACS. High performance tactical-class rocket motors typically have thrust misalignment errors of between 0.15° and 0.25° .³ The misalignment of very small motors can be double this. The needed torque of the ACS to counteract these thrust misalignments is approximately the thrust times the distance between the nozzle of the rocket motor and the center-of-mass of the vehicle times the misalignment error expressed in radians.

As shown in Figure 1, the thrust of SRMs for high ΔV CubeSat applications ranges from 40 to 260 N. The torque experienced by a 30 cm long CubeSat due to SRM misalignment can therefore be as high as $(0.5^\circ)(0.0175 \text{ rad/deg})(260 \text{ N})(0.15 \text{ m})$ or 0.34 N-m. For a CubeSat mass of 3 kg, the pitch/yaw moment of inertia (i.e., the moment of inertia of the length) is about $(1/12)(3 \text{ kg})[(0.1 \text{ m})^2 + (0.3 \text{ m})^2]$ or 0.025 kg-m^2 , so the CubeSat will accelerate at about 780 deg/s^2 when a 260 N motor fires with a 0.5° thrust misalignment.

Attitude thrusters can be used to counteract this unwanted angular acceleration. To do so, their thrust must be on the order of $(0.5^\circ)(0.0175 \text{ rad/deg})(260 \text{ N})$ or 2.3 N and their total impulse must be on the order of 23 N-s (margin not included). This is in addition to the total impulse required for other functions. The maximum thrust version of the mono prop thrusters of Figure 2 can typically provide 2.5 N of thrust at the beginning of life, when the supply pressure (about 500 psi max) is a maximum, and 1 N of thrust at the end of life.⁴ Therefore, a CubeSat mono prop system can provide attitude control for a CubeSat SRM. However, the total mass of a CubeSat mono prop system is typically about 1.5 kg for an 800 N-s system. A mono prop system designed exclusively for CubeSat SRM attitude control might be about 0.5 kg. Adding this mass to the 1 to 1.5 kg of the SRM reduces its propellant mass fraction from a range of 0.5 to 0.7 to a range of 0.3 to 0.5. Therefore, a less massive attitude control solution is desirable.

An alternative to attitude thrusters is thrust vector control (TVC). TVC systems can compensate for thrust misalignments by redirecting the thrust by an appropriate angle relative to the vehicle. Figure 3 illustrates some conventional TVC systems. Conventionally, TVC for rocket-propelled vehicles is performed using jet vanes, a

gimbaled nozzle, a gimbaled engine, multiple engines with variable thrust, or a vectoring exhaust nozzle. Some unconventional approaches are shown in Figure 4, and include fluid injection, axial plates, and jet tabs⁵.

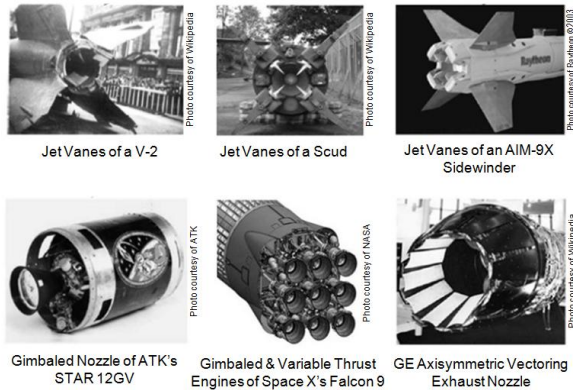


Figure 3: Some Conventional TVC Systems

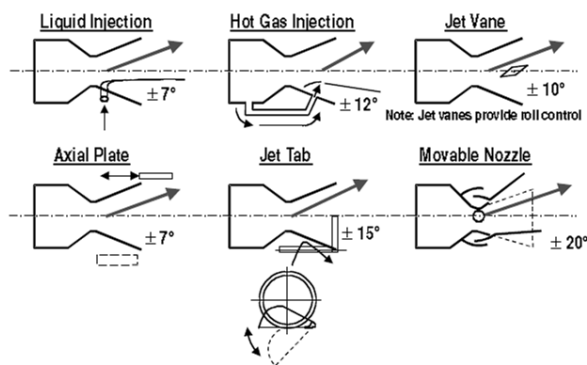


Figure 4: Unconventional (left) and Conventional (right) TVC Systems

Virtually all of the high total impulse CubeSat propulsion systems shown in Figure 2 use multiple thrusters with variable thrust for attitude control. This TVC approach requires a throttleable valve for each thruster. The mass, size and electrical power of these valves scales with thrust, and therefore limits the propellant mass fraction achievable with this approach for high thrust SRMs.

Traditional TVC approaches such as jet vanes and gimbaled nozzles can potentially be scaled down to sizes appropriate for 1 to 10 kg SRMs, but there are many challenges. The dimension of the nozzle is on the order of 1 cm, so components under a centimeter in size must be developed, and they must withstand the very harsh temperature and erosion environment of the SRM exhaust. A TVC approach that does not have to address these challenges may be preferred.

Over the past three years, we have investigated two unconventional approaches to TVC for very small, high thrust propulsion systems such as ~1 kg SRMs. We call these two approaches “movable mass TVC” and “jet paddle TVC”. These two methods are patent pending.

4. TWO TVC SYSTEMS FOR CONTROLLING THE ATTITUDE OF ROCKET-PROPELLED CUBESATS

4.1 Movable Mass

A movable mass is one or more volumes of mass that can be moved to alter the location of the center-of-mass of a vehicle. Movable masses for attitude control have been analyzed and computer simulated for kinetic kill vehicles⁶⁻⁸. However, these movable masses have been internal to these vehicles, and they have not been applied specifically to mitigating thrust misalignments. Our movable mass TVC system is quite different.

When the lines of action of the thrust or other applied forces acting on a vehicle do not pass through the center-of-mass of the vehicle, a torque is created about the center-of-mass. This causes the attitude of the vehicle to change in accordance with the torque. Thus, by moving mass in the vehicle in an appropriate way, the center-of-mass can be moved relative to the lines of action of the forces, and a torque can be generated for attitude control. As the attitude of the vehicle changes, the thrust direction also changes, allowing the vehicle to be steered.

Mass can be moved in a variety of ways -- solenoids, motors, magnetic fields, fluid flow, etc. In the case where magnetic or other force fields are used, movable mass need not be physically attached to the vehicle at all, but instead can be “suspended” using the magnetic or other fields. The quantity, size, distribution, range of motion, speed, and acceleration of the movable mass may be tailored to a specific application. For some applications, the mass, size, and power needs of a movable mass system may be lower than those of a more traditional ACS. This may make a movable mass system particularly suitable for use in small vehicles.

Figure 5 illustrates a rocket-propelled exoatmospheric vehicle where torque is controlled via internal movable masses. In this example, only two dimensions and one force (thrust) are considered for simplicity.

The left image shows the case where the thrust line-of-action is perfectly aligned with the longitudinal axis or axis of symmetry of the vehicle and passes through the center-of-mass. The thrust is denoted T , the mass of vehicle m_V , the relevant moment of inertia I_V , the mass of the “movable mass” m_B , which is typically less than m_V ,

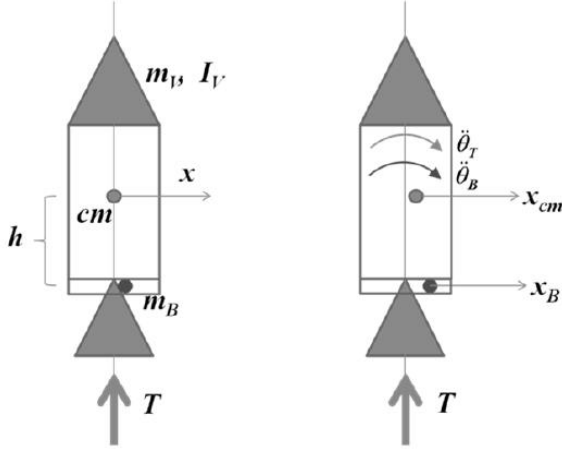


Figure 5: Movable Mass TVC Concept

and the distance from the center-of-mass to the line-of-motion of the movable mass h . The angle θ corresponds to pitch or yaw. For simplicity, the line-of-motion of m_B is orthogonal to the thrust line-of-action. The coordinate in the movable mass line-of-motion direction is x . As the ACS moves m_B an amount x_B , the center-of-mass moves an amount x_{cm} . Two torques are created – one due to the thrust and its lever arm x_{cm} , which corresponds to an angular acceleration $\ddot{\theta}_T$, and another due to the reaction force of the vehicle caused by the acceleration of the movable mass x_B , and its lever arm h , which corresponds to an angular acceleration $\ddot{\theta}_B$. The sum of these two angular accelerations is the net angular acceleration of the vehicle. Once the movable mass stops accelerating, only $\ddot{\theta}_T$ remains. The following equations provide these angular accelerations:

$$x_{cm} = \left(\frac{m_B}{m_V + m_B} \right) x_B \quad (5)$$

$$\ddot{\theta}_T = \frac{T x_{cm}}{I_V + m_B x_B^2} \quad (6)$$

$$\ddot{\theta}_B = \frac{m_B \ddot{x}_B h}{I_V + m_B x_B^2} \quad (7)$$

$$\ddot{\theta}_{NET} = \ddot{\theta}_T + \ddot{\theta}_B \quad (8)$$

The right image of Figure 5 can be considered the case of a thrust misalignment (m_B is initially not moving relative to the vehicle in this case). To nullify the torque due to this thrust misalignment, m_B is moved so that the center-of-mass intersects the line-of-action of the thrust, as shown in the left image. The location and path of m_B shown in Figure 5 is for purposes of illustration only. The location and path of the movable mass can be anywhere (i.e., inside, outside, and/or inside and outside of the vehicle), provided it is attached or otherwise affixed (e.g., via magnetic fields) to the vehicle and changes the center-of-mass location of the vehicle. The quantity of mass that

is moved, the path over which the mass moves, and the speed and acceleration with which the mass is moved depend on the requirements of the ACS and the desired attitude correction. Roll can also be controlled if a force that is not parallel to the roll axis is acting on the vehicle, such as a lift or drag force in endoatmospheric flight, or any other suitable force.

A significant feature of the movable mass TVC approach is its scalability with the mass and size of the vehicle. Generally speaking, the mission requirements of spacecraft and other similar vehicles include kinematic parameters such as translational and angular accelerations. As the mass of a vehicle is reduced, the forces and torques required to achieve these accelerations are also reduced. The quantity of movable mass required to shift the center of mass and achieve a specified level of attitude control authority is also reduced proportionately. Since there are a wide range of miniature actuators available for moving mass, the movable mass TVC approach can be very small and may be appropriate for very small vehicles.

4.2 Jet Paddles

Figure 6 illustrates a two jet paddle TVC system. Jet paddles are thin rectangular plates or slabs with a face exposed to the exhaust flow and are located just aft of the nozzle of the rocket motor. The jet paddles typically pivot about their edge closest to the exit of the nozzle in a manner that rotates them into and out of the exhaust flow. When the jet paddles are rotated away from the exhaust flow, they do not affect the exhaust flow, and no thrust vectoring occurs.

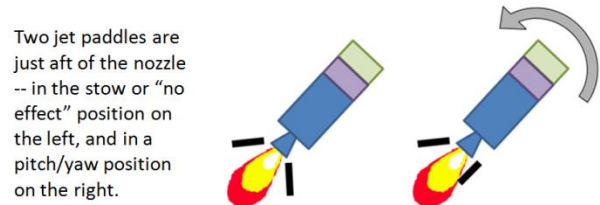
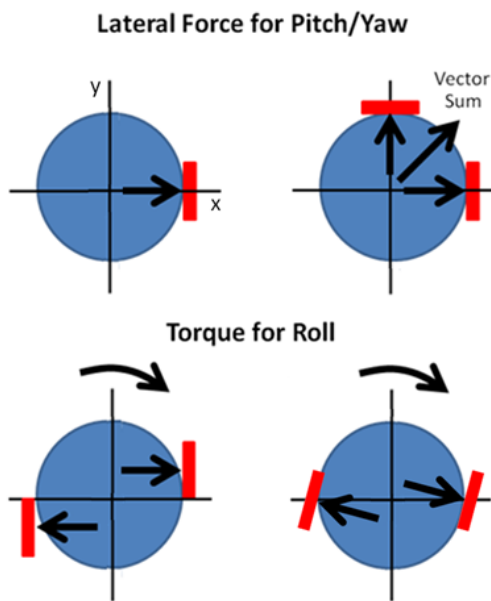


Figure 6: Jet Paddle TVC Concept

However, when a single jet paddle is moved near the flow, as shown on the right in Figure 6, the rotated jet paddle, in effect, forms an asymmetric extension of the nozzle. Since the exhaust pressure on the rotated jet paddle is greater than that on the opposite jet paddle, a lateral force is created, and the vehicle rotates about its center-of-mass as shown. In this case, the rotation of the top of the vehicle is to the left. There are two ways to remove the lateral force: (1) move the jet paddle in the exhaust flow back away from the exhaust flow; or (2)

move the opposite jet paddle into the exhaust flow to create an equal, but opposite, lateral force.

Figure 7 illustrates jet paddle configurations to create various vehicle rotations. The x-axis and y-axis lines are orthogonal to one another and are also orthogonal to and intersect the axis of symmetry of the respective nozzles of each configuration. The jet paddles are thin rectangular plates or slabs with their faces parallel to the axis of symmetry of the nozzle, which is normal to the page. The view is looking down into an exhaust nozzle and seeing the bottom edge of the jet paddles (i.e., the edge farthest from the nozzle exit). It is assumed in Figure 7 that the axis of symmetry of the nozzle passes through the center-of-mass of the vehicle.



The view is looking into the nozzle (blue) and seeing the bottom edge of the paddles (red).

Figure 7: Achievable Vehicle Rotations using Jet Paddles

In the configuration shown on the top-left, the face of a single paddle is centered relative to the center of the nozzle. The paddle creates a lateral force having a line-of-action that intersects the axis of symmetry of the nozzle. This force can be used to pitch or yaw a vehicle, i.e., to rotate a vehicle about an axis that is orthogonal to the axis of symmetry of the nozzle, e.g., the x-axis or y-axis.

In the configuration shown in the top-right, a second paddle is added around the nozzle. This creates a second lateral force orthogonal to the first lateral force from the first paddle. The vector sum of the forces (i.e., the total

lateral force) is directed between the paddles as shown. By varying the magnitude of each lateral force (e.g., by changing the distance between the respective paddle and the exhaust flow), the total lateral force can be in any direction between the two paddles. This effect can be used to create any desired combination of pitch and yaw for a vehicle.

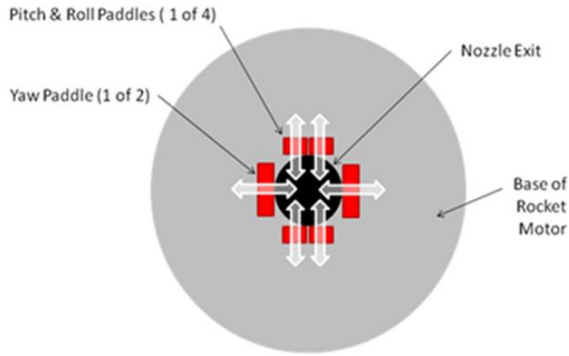
In the configuration in the bottom-left, two opposing paddles are positioned kitty-corner to one another about the nozzle so the normal of their faces misses the axis of symmetry of the nozzle by the same distance. This paddle placement creates equal and opposite lateral forces equally spaced from the axis of symmetry of the nozzle, which causes the vehicle to roll (i.e., rotate about the axis of symmetry of the nozzle).

In the configuration shown on the bottom-right, two opposing paddles “twist” to create a roll torque. The twist is about each paddle’s axis of symmetry parallel to the axis of symmetry of the nozzle. As in the adjacent configuration to the left, equal and opposite forces equally spaced from the axis of symmetry of the nozzle cause the vehicle to roll.

In each case, how far each paddle is moved, and which paddles are moved, will control both the type of rotation that the vehicle experiences and the amount of rotation. Multiple types of control may be applied at the same time.

Figure 8 illustrates a six jet paddle TVC system capable of controlling pitch, yaw, and roll. The jet paddles are assumed to be thin rectangular slabs or plates with one side facing the axis of symmetry of the nozzle, as described above with respect to Figure 7. As with Figure 7, the view is looking into the nozzle. The white arrows illustrate the direction of the jet paddles into and out of the flow. A hinge may be located along the top edge of each of the jet paddles, i.e., the edge closest to the base of rocket motor so the jet paddles can be rotated into and out of the flow. Alternatively, the jet paddles may not rotate, but may be translated into and out of the flow in the direction of the arrows. Other methods of moving the jet paddles into and out of the flow are possible.

Any desired motive mechanism can be used to move the jet paddles into and out of the exhaust flow, e.g., electrical actuators, hydraulic actuators, pneumatic actuators, a combination thereof, etc. The shape, thickness, and composition of jet paddles can be tailored to the specific application. Jet paddles and their actuators can be permanently attached to the vehicle, or can be designed to be removable and reusable. The jet paddle approach is scalable; it can be used on very small and very large rocket motors.



The view is looking into the nozzle and seeing the bottom edge of the paddles. The actuator for each paddle is not shown. For the orientation shown, a face of each jet paddle (red) is parallel to the axis of symmetry of the rocket nozzle (black). The white arrows illustrate the direction in which the paddles move.

Figure 8: Pitch, Yaw and Roll Control using 6 Jet Paddles

In principle, the use of jet paddles is similar to using jet vanes, but has distinct advantages. One significant advantage is that jet paddles have considerably less exposure to the hot gases and particulates of the exhaust flow. Stagnation temperatures of 3,310-3,588 K, or 5,500-6,000 °F, are typical in conventional jet vane systems. This restricts the composition of jet vanes to materials that can be exposed to a high temperature, such as graphite, rhenium, tungsten-copper, or tungsten carbide/stainless steel. Since jet paddles need not be continuously and directly in the exhaust flow and therefore need not have a stagnation point, the heating and erosion environment for jet paddles is an order of magnitude less than that for jet vanes. Consequently, a jet paddle may be made of a wider variety of materials, such as iron, steel, stainless steel, various ceramics, etc.

Another advantage of jet paddles relative to jet vanes is the design freedom available for their size and shape. The nozzle exit diameter imposes restrictions on the size of jet vanes. Due to the difference in orientations and locations, this is not the case for jet paddles. The length of a jet paddle is essentially unconstrained, and hence, its surface area is also essentially unconstrained. This affords significant flexibility in jet paddle shape and size, and therefore performance.

Another significant advantage of the jet paddle TVC approach is its scalability with the size of the vehicle. The thrust of a vehicle designed for a particular mission generally scales with its size. Since the size of jet paddles and the force needed to operate their actuators generally

scales with the thrust, the wide variety and availability of very small actuators enables jet paddle TVC systems to scale with the size of the vehicle.

5. PROOF-OF-CONCEPT FLIGHT DEMONSTRATIONS

5.1 Movable Mass

A proof-of-concept flight vehicle was designed, fabricated, and flown to demonstrate the movable mass TVC concept. Figure 9 is a solid-model rendering of this vehicle. The vehicle consists of a 1 kg CubeSat, a 1 kg SRM, and an external movable mass pitch/yaw TVC system using four rotating arms. The CubeSat payload includes the parachute, sensors, computing system, and battery to fly and operate the vehicle. The rocket motor is the ISP 30 sec Motor shown in Figure 1. The mass of each arm with its end mass is 3.7% of the total mass of the vehicle, or about 75 grams. The mass of a single arm and its servo is about 90 grams. Therefore, the mass of the movable mass TVC system is about 18% of the total mass of vehicle. Since this is a proof-of-concept vehicle, the TVC system was designed with substantial thrust-misalignment margin. The TVC system is capable of handling up to 1.7° of thrust misalignment (about 10 times that of tactical solid rocket motors). Since the thrust misalignment is generally much less than 1.7°, the vehicle has an ample amount of attitude control and steering authority. The mass of the arms scales proportionately with the thrust, the thrust misalignment and desired attitude control authority, and the vehicle mass (without arms). The mass of the four arms can be reduced from 300 grams to 90 grams if the maximum expected thrust misalignment is 0.5° rather than 1.7°. The total mass of the moving mass TVC system would then be about 150 grams. Each arm servo is powered at 5 V and consumes about 5 W under load. Each arm can rotate at a maximum speed of 225 deg/sec (under load).

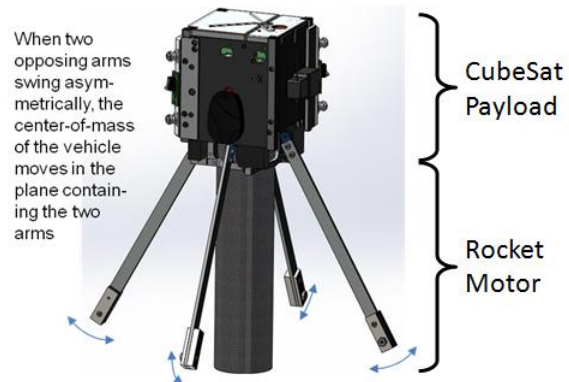


Figure 9: Moving Mass TVC System Proof-of-Concept Vehicle

Figure 10 provides a photograph of the actual proof-of-concept vehicle, and also a photograph of this vehicle about 1 sec after launch of its maiden flight test, which occurred on June 28, 2012. The rocket motor was designed to burn for 7 sec and provide 60 N of thrust during this flight. The movable mass pitch/yaw TVC system was commanded by a 50 Hz update rate control loop that provided full pitch/yaw control while the vehicle was thrusting. This flight demonstrated that a movable mass pitch/yaw TVC system can effectively control the pitch/yaw of small rocket vehicles.



Figure 10: Moving Mass TVC Proof-of-Concept Flight Vehicle and Test Flight

5.2 Jet Paddles

A proof-of-concept flight vehicle was also designed, fabricated, and flown to demonstrate the jet paddle TVC concept. Figure 11 is a photograph of this vehicle. The vehicle consists of a 1 kg CubeSat, a 1 kg SRM, and a jet paddle TVC system using 8 jet paddles. The CubeSat and SRM are the same as described above, but the SRM used a cleaner burning propellant. The vehicle has four legs to hold it upright for display and for protecting the jet paddles from damage due to the landing of a test flight.

The 8 jet paddle TVC system is attached to the bottom of the rocket motor. Each Inconel™ paddle is approximately 2.5 cm long x 0.64 cm wide x 1.3 mm thick (1 inch long x 0.25 inch wide x 0.05 inch thick). Pairs of paddles are positioned next to one another and separated by a small gap. The paddles can be moved into and out of the flow by a respective linkage connected to a respective electrically powered rotary servo. Each servo is powered at 5 V and consumes about 2 W under load. Each paddle can rotate at a maximum speed of

1350 deg/sec (under load). The paddles are shown in their stow position in Figure 11, 30° away from the axis of symmetry of the nozzle. When rotated 10° into the flow relative to the axis of symmetry of the nozzle, each paddle can generate a lateral force of approximately 4 N (for 60 N of thrust), which is equivalent to a 3.8 deg thrust vector angle. The complete jet paddle assembly (paddles, linkages, servos, and attachment hardware) has a mass of 150 grams.

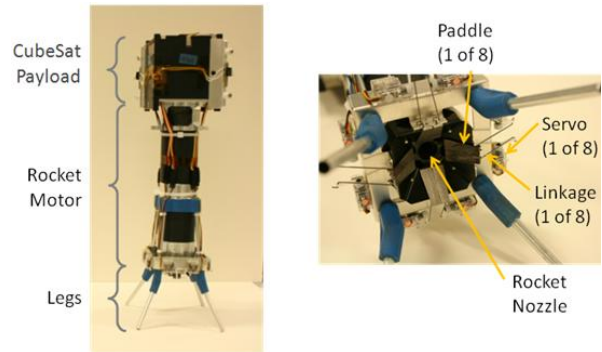


Figure 11: Jet Paddle TVC Proof-of-Concept Flight Vehicle

The proof-of-concept flight vehicle flew a test flight on August 28, 2013, which is shown in Figure 12. The jet paddle TVC system was commanded by a 50 Hz update rate attitude control loop that provided full attitude control of the vehicle while it was thrusting. The jet paddles showed no sign of thermal or erosion damage after the flight. This flight demonstrated that a jet paddle TVC system can effectively control the attitude of small rocket vehicles.



Figure 12: Jet Paddle TVC Proof-of-Concept Flight Vehicle and Test Flight

6. CONCLUSIONS AND FUTURE PLANS

The availability of small, light-weight TVC systems such as the moving mass TVC system and the jet paddle TVC system opens up new applications for small high-thrust SRMs. One of these applications is providing large amounts of ΔV to CubeSats in a relatively short period time – seconds for SRMs as compared to hours for mono prop systems and days for electric systems.

For example, ATK's STAR 4G motor (1.4U x 1.5 kg) shown in Figure 1, coupled with a TVC system that increases its initial mass by 20%, has a total impulse per unit volume comparable to the largest values in Figure 2, and can provide a 3 kg CubeSat payload a ΔV of 620 m/s, which is 160 m/s, or 35%, more ΔV than the largest ΔV shown in Figure 2. This is sufficient ΔV for a roughly 1250 km change in LEO orbital altitude. Since a Hohmann Transfer to a new orbit requires two motor burns, a two-pulse motor, or a restartable hybrid motor, or at least two motor stages, is required.

If the payload is a smaller CubeSat of 1 kg, the ΔV increases to 1170 m/s, sufficient to raise or lower the CubeSat altitude by 2700 km, or to achieve a LEO plane change of about 9 deg. If the motor is scaled down to a volume of 1U (and 1 kg), the ΔV is about 950 m/s. If the motor is scaled up to a volume of 2U (2.5 kg) the ΔV is about 1400 m/s. If the payload mass is increased to 10 kg and coupled with the baseline 1.4U x 1.5 kg motor, the ΔV is 235 m/s, sufficient for a 435 km change in LEO altitude.

In addition to LEO maneuvers, another application may be the transfer of CubeSats from LEO-to-GEO using a relatively small and lightweight two-stage or three-stage transfer vehicle. Future research at The Aerospace Corporation will investigate this possibility.

Acknowledgements

The Aerospace Corporation's Technical Investment Program is acknowledged and thanked for funding the work described in this paper.

References

1. Wertz, J.R. and Larson, W.J., Space Mission Analysis and Design, 3rd Edition, Kluwer Academic Publishers, Netherlands, 1991.
2. Hargus, W.A. and Singleton, J.T., "Annual Assessment of CubeSat Propulsion Technology and Maturity," Proceedings of the 6th Government CubeSat Technical Interchange Meeting, Pasadena, CA, April 2014.

3. Knauber, R.N., "Thrust Misalignments of Fixed-Nozzle Solid Rocket Motors," Paper 95-2874, AIAA/ASME/SAE/ASEE 31st Joint Propulsion Conference, San Diego, CA, 10-12 July 1995.
4. Schmuland, D.T., Masse, R.K., Sota, C.G., "Hydrazine Propulsion Module for CubeSats," Proceedings of the 25th Annual AIAA/USU Conference on Small Satellites, Logan, UT, 2011.
5. Fleeman, E.L., Tactical Missile Design, 2nd Edition, AIAA, 2006.
6. Menon, P.K., Sweriduk, G.D., Ohlmeyer, E.J., Malyevac, D.S., "Integrated Guidance and Control of Moving Mass Actuated Kinetic Warheads," Proceedings of the 11th Annual AIAA/MDA Technology Conference, 29 July - 2 August 2002, and AIAA Journal of Guidance, Control and Dynamics, Volume 27, Issue 1, 2004.
7. Menon, P.K., Vaddi, S.S., Ohlmeyer, E.J., "Finite-Horizon Robust Integrated Guidance-Control of a Moving-Mass Actuated Kinetic Warhead," Proceedings of the AIAA Guidance, Navigation, and Control Conference, 21-24 August 2006.
8. Vaddi, S.S., Menon, P.K., Ohlmeyer, E.J., "Numerical State-Dependent Riccati Equation Approach for Missile Integrated Guidance Control," Proceedings of the AIAA Guidance, Navigation, and Control Conference, 20-23 August 2007, and AIAA Journal of Guidance, Control, and Dynamics, Volume 32, Issue 2, 2009.

NOTE: All trademarks, trade names, and service marks are the property of their respective owners.